

Optimized quantum singular value thresholding algorithm based on a hybrid quantum computer

Yangyang Ge(葛阳阳), Zhimin Wang(王治旻), Wen Zheng(郑文), Yu Zhang(张钰), Xiangmin Yu(喻祥敏), Renjie Kang(康人杰), Wei Xin(辛蔚), Dong Lan(兰栋), Jie Zhao(赵杰), Xinsheng Tan(谭新生), Shaoxiong Li(李邵雄), and Yang Yu(于扬)

Citation: Chin. Phys. B, 2022, 31 (**4**): 048704. DOI: 10.1088/1674-1056/ac40fb
Journal homepage: http://cpb.iphy.ac.cn; http://iopscience.iop.org/cpb

What follows is a list of articles you may be interested in

Quantum walk search algorithm for multi-objective searching with iteration auto-controlling on hypercube

Yao-Yao Jiang(姜瑶瑶), Peng-Chen Chu(初鹏程), Wen-Bin Zhang(张文彬), and Hong-Yang Ma(马鸿洋)
Chin. Phys. B, 2022, 31 (**4**): 040307. DOI: 10.1088/1674-1056/ac2806

Quantum watermarking based on threshold segmentation using quantum informational entropy

Jia Luo(罗佳), Ri-Gui Zhou(周日贵), Wen-Wen Hu(胡文文), YaoChong Li(李尧翀), and Gao-Feng Luo(罗高峰)
Chin. Phys. B, 2022, 31 (**4**): 040302. DOI: 10.1088/1674-1056/ac2803

Quantum partial least squares regression algorithm for multiple correlation problem

Yan-Yan Hou(侯艳艳), Jian Li(李剑), Xiu-Bo Chen(陈秀波), and Yuan Tian(田源)
Chin. Phys. B, 2022, 31 (**3**): 030304. DOI: 10.1088/1674-1056/ac1b84

Low-loss belief propagation decoder with Tanner graph in quantum error-correction codes

Dan-Dan Yan(颜丹丹), Xing-Kui Fan(范兴奎), Zhen-Yu Chen(陈祯羽), and Hong-Yang Ma(马鸿洋)
Chin. Phys. B, 2022, 31 (**1**): 010304. DOI: 10.1088/1674-1056/ac11cf

Image reconstruction from few views by l_0-norm optimization

Sun Yu-Li, Tao Jin-Xu
Chin. Phys. B, 2014, 23 (**7**): 078703. DOI: 10.1088/1674-1056/23/7/078703

Optimized quantum singular value thresholding algorithm based on a hybrid quantum computer

Yangyang Ge(葛阳阳), Zhimin Wang(王治旻), Wen Zheng(郑文), Yu Zhang(张钰), Xiangmin Yu(喻祥敏), Renjie Kang(康人杰), Wei Xin(辛蔚), Dong Lan(兰栋), Jie Zhao(赵杰), Xinsheng Tan(谭新生), Shaoxiong Li(李邵雄)†, and Yang Yu(于扬)‡

National Laboratory of Solid State Microstructures, School of Physics, Nanjing University, Nanjing 210093, *China*

(Received 31 October 2021; revised manuscript received 23 November 2021; accepted manuscript online 8 December 2021)

Quantum singular value thresholding (QSVT) algorithm, as a core module of many mathematical models, seeks the singular values of a sparse and low rank matrix exceeding a threshold and their associated singular vectors. The existing all-qubit QSVT algorithm demands lots of ancillary qubits, remaining a huge challenge for realization on near-term intermediate-scale quantum computers. In this paper, we propose a hybrid QSVT (HQSVT) algorithm utilizing both discrete variables (DVs) and continuous variables (CVs). In our algorithm, raw data vectors are encoded into a qubit system and the following data processing is fulfilled by hybrid quantum operations. Our algorithm requires $O[\log(MN)]$ qubits with $O(1)$ qumodes and totally performs $O(1)$ operations, which significantly reduces the space and runtime consumption.

Keywords: singular value thresholding algorithm, hybrid quantum computation

PACS: 87.55.kd, 03.67.Ac **DOI:** 10.1088/1674-1056/ac40fb

1. Introduction

Quantum computation,[1] since its quantum advantage over conventional one, has been an attractive and inspiring field for decades. Many physical platforms, such as trapped ions,[2–4] nuclear magnetic resonance,[5,6] photons,[7–9] and solid state superconducting devices[10–13] have been deeply explored to find a viable way to building a quantum computer. While the major effort has been put on the quantum operations on two-state quantum variables (being known as qubits), for quantum systems, there exist both DVs and CVs. Resources like position, momentum, and quadrature amplitudes of the electromagnetic field are suitable candidates for continuous variables. The quantum version of a CV mode (qumode)[14] can be comparable to a qubit. The quantum information processing can take advantage of both DVs and CVs.[15,16] Its superiority has been shown in applications like quantum float computing[17] and quantum phase estimation.[1,14]

In this paper, by using both DVs and CVs, we propose a hybrid quantum algorithm for singular value thresholding (SVT) to efficiently save physical resources while with quantum speed-up. SVT is a core module in many important applications like computer vision and machine learning. Specifically, the SVT algorithm has been applied to solve many nuclear norm minimizing (NNM)-based problems, such as matrix completion, matrix denoising, and principle component analysis (PCA).[18–20] The processes of SVT are the main computational cost for those applications.

Since the superiority of quantum computer, many remarkable quantum machine learning[21] algorithms have been proposed. A QSVT algorithm[22,23] has been developed that can execute the SVT operator exponentially faster than its classical counterparts. The algorithm for QSVT consists of three main parts: quantum phase estimation, Newton iteration, and controlled rotation. All the three parts require indispensable ancillary qubits as registers for quantum float computing. Depend on the desired precision, the demand for the number of ancillary qubits could be large and a grand challenge for realization on near-term intermediate-scale quantum computers. This motivates us to resort to hybrid quantum computation and work out a more efficient approach to economize the quantum resources.

Vectors of classical data are better encoded in quantum states of qubit systems, as each component of a vector now becomes the corresponding amplitude directly. However, the all-qubit approach demands for lots of ancillary qubits as registers in its several main parts, which can be more efficiently performed with CVs-based operations. Given the above two considerations, it naturally calls for a hybrid quantum computing approach that exploits both the advantages of qubits and qumodes, as would be explored in this paper.

In our proposed hybrid QSVT algorithm, singular values are encoded into the CVs and singular value transformation can be implemented by hybrid controlled unitary transformations. In contrast to the all-qubit scheme that requires redundant qubits and complicated circuits, our hybrid scheme consumes only a limited amount of qubits and qumodes and significantly reduces the complexity of the circuit. Our complexity analysis shows that the hybrid scheme depresses the order

†Corresponding author. E-mail: shaoxiong.li@nju.edu.cn
‡Corresponding author. E-mail: yuyang@nju.edu.cn

© 2022 Chinese Physical Society and IOP Publishing Ltd

of runtime comparing the all-qubit approach.

The remainder of this paper is organized as follows: We give a brief review of the all-qubit QSVT algorithm in Section 2 and propose our modified hybrid QSVT algorithm in Section 3. Section 4 analyzes the complexity, success probability, and fidelity. We present our conclusions in Section 5.

2. All-qubit QSVT algorithm

In this section, we first briefly review the procedures of the all-qubit QSVT algorithm. And then design a modified hybrid QSVT algorithm (HQSVT).

The QSVT algorithm is based on the singular value decomposition (SVD).[18] Given a low rank matrix $A \in R^{M\times N}$ with rank $R \leq \min(M,N)$, $A_{i,j}$ represents the elements of the i-th row and j-th column of matrix A. The singular value decomposition (SVD) of A is a factorization $A = U\Sigma V^* = \sum_{k=1}^{R} \sigma_k \boldsymbol{u}_k \boldsymbol{\nu}_k$, where σ_k are called singular values of A and $\boldsymbol{u}_k$, $\boldsymbol{\nu}_k$ represent left and right singular vectors respectively. In the QSVT algorithm, suppose the matrix A is the input, the output takes the form of $\sum_{k=1}^{r}(\sigma_k-\tau)_+\boldsymbol{u}_k\boldsymbol{\nu}_k$ where $r \leq R$ and τ is a threshold. Here $(\sigma_k-\tau)_+ = \max(\sigma_k-\tau,0)$.

Figure 1 shows the circuit representation of the QSVT algorithm. The algorithm is based on the HHL algorithm[24] and can be decomposed into five parts. The state evolution corresponds to each part of the circuit is represented in Fig. 2. In initialization, by using quantum random access memory (qRAM),[25–27] the elements of the input matrix A are stored in register B. In the first part, the algorithm performs the quantum phase estimation $\hat{U}_{\rm PE}$ and stores the singular value information in register C. The second part contains an unitary operation $\hat{U}_{\sigma,\tau}$ which converts the eigenvalues $|\sigma_k^2\rangle$ stored in register C to the intermediate result $|y_k\rangle$ stored in the register L, where $y_k = (1-\tau/\sigma_k)_+ \in [0,1)$. Then $|y_k\rangle$ stored in register L containing the information of eigenvalues is assigned to the amplitude of the auxiliary qubit through rotation transformation in the third step. In the fourth part, an unitary transformation $\hat{U}^\dagger$ is used to eliminate the unwanted registers. Eventually, the measurement is performed on the auxiliary qubit and register B collapses to the target quantum state. The algorithm outputs the state $|\psi_S\rangle$ close to the desired result.

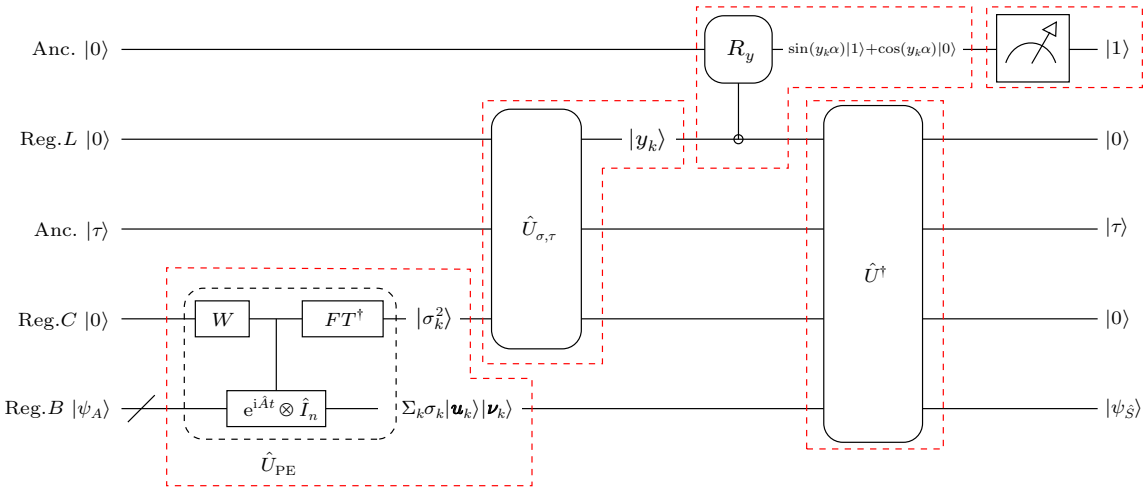


Fig. 1. Quantum circuit of the all-qubit QSVT algorithm. The circuit is divided into 5 parts by the red dashed box. The bottom wire with '/' represents a group of qubits.

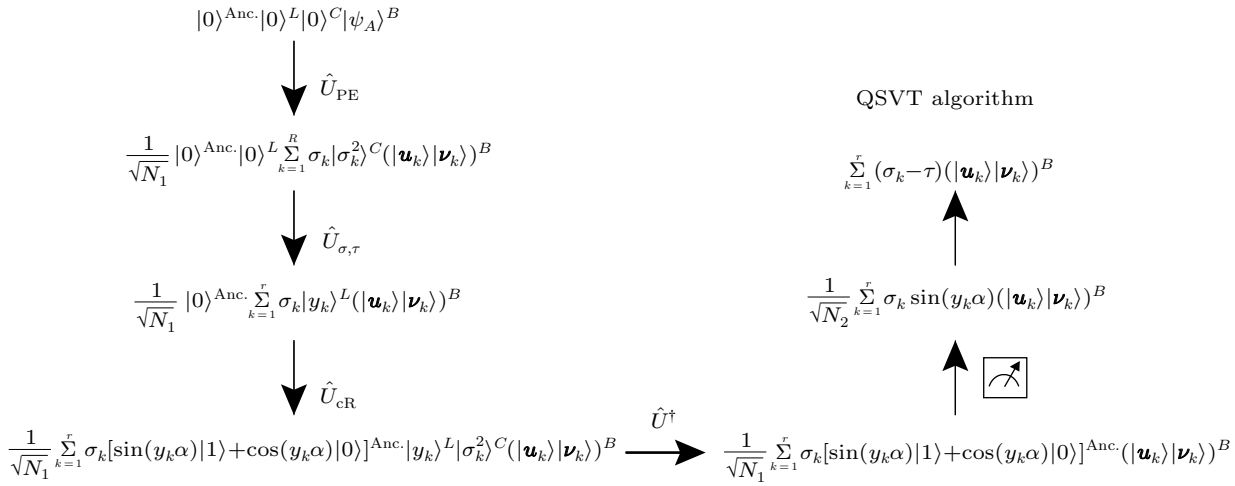


Fig. 2. Entire state evolution corresponding to procedures of the all-qubit QSVT algorithm. The ancillary state $|\tau\rangle$ is omitted because it remains the same during the evolution of the quantum circuit.

3. Hybrid QSVT algorithm

In this section, we elaborate our modified hybrid QSVT algorithm (HQSVT). For the all-qubit QSVT algorithm, it can be decomposed into several main procedures, including quantum phase estimation, Newton iteration, and controlled rotation. We keep these procedures and reconstruct them with hybrid operations or CVs-based operations.

The first reconstructed procedure of our algorithm is quantum phase estimation, where a hybrid operator $\hat{U} = \mathrm{e}^{-\mathrm{i}A^{\mathrm{T}}A\hat{P}}$ is constructed to extract the singular values and register them into the qumode. As shown in Eq. (1),

$$\begin{aligned} & \mathrm{e}^{-\mathrm{i}H\hat{P}t}\,|\psi\rangle\,|0\rangle_q \\ &= \mathrm{e}^{-\mathrm{i}\sum_j E_j|\Phi_j\rangle\langle\Phi_j|\hat{P}t}\sum_j \psi_j\,|\Phi_j\rangle\,|0\rangle_q \\ &= \sum_j \mathrm{e}^{-\mathrm{i}E_jt\hat{P}}\psi_j\,|\Phi_j\rangle\,|0\rangle_q \\ &= \sum_j \psi_j\,|\Phi_j\rangle\,|E_jt\rangle. \end{aligned} \tag{1}$$

The operator $\hat{U} = \mathrm{e}^{-\mathrm{i}H\hat{P}}$ with $H = A^{\mathrm{T}}A$ is applied on state $|\psi\rangle\,|0\rangle_q$ and the result takes the form of $\sum_i \psi_i\,|E_i\rangle\,|E_it\rangle$, where $|E_i\rangle$ is the eigenstate of H and $|0\rangle_q$ is a qumode in the initial state as a register. The registering of singular values is equivalent to the add operation, with the quantity of addition depends on the eigenvalues of H. Now the problem becomes how to construct the density matrix exponentiation of $A^{\mathrm{T}}A\hat{P}$.[19] Note that

$$\mathrm{Tr}_\rho\left(\mathrm{e}^{-\mathrm{i}\delta tS_{\mathrm{m}}}\rho\otimes\rho'\mathrm{e}^{\mathrm{i}\delta tS_{\mathrm{m}}}\right) = \mathrm{e}^{-\mathrm{i}\delta t\rho}\rho'\mathrm{e}^{\mathrm{i}\delta t\rho} + O(\delta t^2). \tag{2}$$

Repeatedly apply the exponential swap operation and trace out ρ, we obtain the density matrix exponentiation $\mathrm{e}^{\mathrm{i}\rho t}$ of density matrix $\rho = A^{\mathrm{T}}A$. Here $A^{\mathrm{T}}A$ has been normalized with $A^{\mathrm{T}}A = A^{\mathrm{T}}A/\mathrm{Tr}(A^{\mathrm{T}}A)$ and S_{m} is the swap operator. To construct $\hat{U} = \mathrm{e}^{-\mathrm{i}A^{\mathrm{T}}A\hat{P}}$, the exponential swap operator should be modified as $\mathrm{e}^{-\mathrm{i}\delta t\hat{P}S_{\mathrm{m}}}$. We now have

$$\begin{aligned} & \mathrm{Tr}_\rho\left(\mathrm{e}^{-\mathrm{i}\delta t\hat{P}S_{\mathrm{m}}}\rho\otimes\rho'\mathrm{e}^{\mathrm{i}\delta t\hat{P}S_{\mathrm{m}}}\right) \\ &= 1 - \mathrm{i}[\rho\hat{P},\rho']\delta t + O(\delta t^2) \\ &= \mathrm{e}^{-\mathrm{i}\delta t\rho\hat{P}}\rho'\mathrm{e}^{\mathrm{i}\delta t\rho\hat{P}} + O(\delta t^2). \end{aligned} \tag{3}$$

By setting $\rho = A^{\mathrm{T}}A$ we obtain $\mathrm{e}^{\mathrm{i}\delta tA^{\mathrm{T}}A\hat{P}}$. Constructing $\hat{U}$ with desired precision ε requires $O(\varepsilon^{-1})$ copies of ρ.[28]

The second reconstructed procedure of our HQSVT algorithm is $\hat{U}_{\sigma,\tau}$. The detailed quantum circuit design of $\hat{U}_{\sigma,\tau}$ can be divided into two parts. The first part is Newton iteration, which can be implemented by computing the functions: $z_k = z(\sigma_k^2) = 1/\sqrt{\sigma_k^2}$ and $y_k = 1 - \tau z_k$. Obviously, it can be done by the basic operations: addition, multiplication,[29] and shift operations. Since universal quantum computation for polynomial transformations of continuous variables effectively allows one to perform quantum floating point manipulations on those variables, here we introduce the CVs-based basic operations to replace the original operations in the all-qubit scheme, which can dramatically decrease the number of qubits needed in the indispensable ancilla registers. As shown in Fig. 3(a), the addition operation uses two qumodes, with state $|a\rangle_{q_1}|b\rangle_{q_2}$ as the input and $|a\rangle_{q_1}|a+b\rangle_{q_2}$ the output. The addition operator takes the form of $\mathrm{e}^{-\mathrm{i}\hat{X}^1\hat{P}^2}$, with the quantity of addition determined by the first qumode $|a\rangle_{q_1}$. The application of three-variable multiply operator $\mathrm{e}^{-\mathrm{i}\hat{X}^1\hat{X}^2\hat{P}^3}$ shown in Fig. 3(b) allows one to multiply X^1 and X^2 and register the result in X^3.

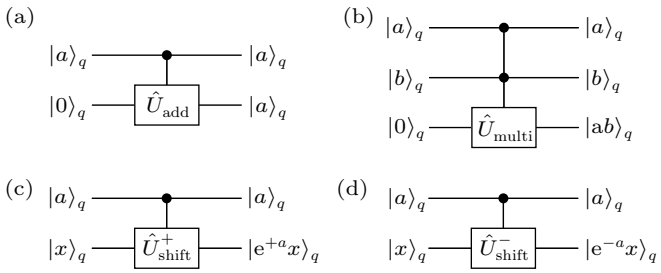


Fig. 3. Addition, multiplication, and shift operations based on CVs. Here we use subscript q to indicate that the register is a qumode. (a) The addition operation needs two qumodes with the first qumode determining the quantity of addition and the second qumode taking the form of output. (b) The multiplication operator multiplies the values stored in the first two qumodes and register the result in the third qumode. Both panels (c) and (d) are shift operations. Here panel (c) takes $Xx \to \mathrm{e}^{+a}Xx$: U^+_{shift} "stretches" Xx and panel (d) takes $Xx \to \mathrm{e}^{-a}Xx$: U^-_{shift} "squeezes" Xx.

Figures 3(c) and 3(d) show the shift operation, with the application of Hamiltonian $+S = (XP+PX)/2$ and $-S = -(XP+PX)/2$, the operator $\hat{U}^+_{\mathrm{shift}} = \mathrm{e}^{-\mathrm{i}(+S)t}$ "stretches" X by the amount of e^t and $\hat{U}^-_{\mathrm{shift}} = \mathrm{e}^{-\mathrm{i}(-S)t}$ "squeezes" P by the amount of e^{-t}.[17] One Newton iteration composed of the above CVs-based basic operations is shown in Fig. 5.[22] The Newton iteration function applied to the function $f(z_k) = 1/{z_k}^2 - {\sigma_k}^2$ is

$$\begin{aligned} z_k^{(i+1)} &= g\left(z_k^{(i)}\right) = z_k^{(i)} - \frac{f\left(z_k^{(i)}\right)}{f'\left(z_k^{(i)}\right)} \\ &= \frac{1}{2}\left(3z_k^{(i)} - \sigma_k^2\left(z_k^{(i)}\right)^3\right). \end{aligned} \tag{4}$$

The next part is the controlled rotation. Here we introduce a hybrid rotation operation shown in Fig. 4, which extracts the y_k stored in register L to the amplitude of the ancilla qubit. The operator $\mathrm{e}^{-\mathrm{i}\hat{X}\otimes\hat{\sigma}_{\mathrm{y}}t}$ is essentially hybrid. It extracts the y_k stored in the qumode and then assigns y_k to the amplitude of an auxiliary qubit, instead of extracting y_k from register L consisting of qubits:

$$\mathrm{e}^{-\mathrm{i}\hat{X}\otimes\hat{\sigma}_{\mathrm{y}}t}|y_k\rangle_q\,|0\rangle = |y_k\rangle_q\left(\cos(y_kt)|0\rangle + \sin(y_kt)|1\rangle\right). \tag{5}$$

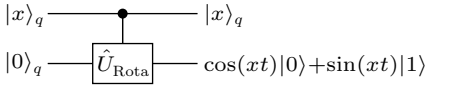


Fig. 4. Circuit of the controlled rotation operation. In this hybrid operation, the value stored in the qumode is assigned to the amplitude of the auxiliary qubit.

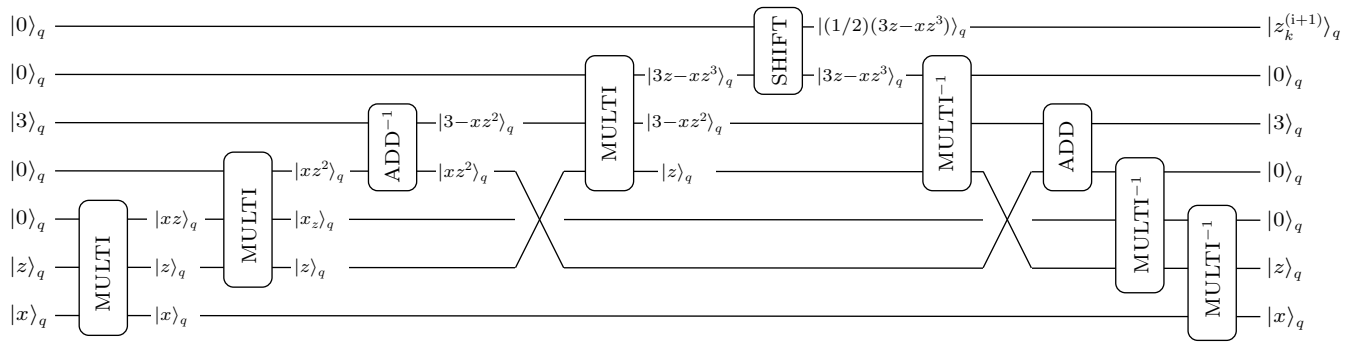


Fig. 5. Quantum circuit of one Newton iteration for computing $z_k^{(i+1)} = g\left(z_k^{(i)}\right) = (1/2)\left(3z - xz^3\right)$. The iteration is composed of CVs-based quantum operations.

The other procedures are consist with the all-qubit scheme. We perform an operator $\hat{U}^\dagger$ and then do the measurement on the auxiliary qubit.

The overall procedures of our HQSVT algorithm is organized as the following steps.

Step 1 Initialization. The matrix A is loaded as state $|\psi_A\rangle$ via qRAM:

$$|\psi_1\rangle = |0\rangle^{\text{Anc.}}|0\rangle_q^L|0\rangle_q^C|\psi_A\rangle^B. \tag{6}$$

Step 2 Quantum phase estimation. Perform $\hat{U} = I \otimes \hat{U}_{\text{PE}}$ on $|\psi_1\rangle$ to get

$$|\psi_2\rangle = \frac{1}{\sqrt{N_0}}|0\rangle^{\text{Anc.}}|0\rangle_q^L \sum_{k=1}^{R} \sigma_k |\sigma_k{}^2\rangle_q^C (|\boldsymbol{u}_k\rangle|\boldsymbol{\nu}_k\rangle)^B, \tag{7}$$

where $N_0 = \sum_{k=1}^{R} \sigma_k^2$.

Step 3 If $\sigma_k \geq \tau$, we perform $\hat{U}_{\sigma,\tau}$ to transform singular values σ_k into y_k and register them into the qumode L,

$$|\psi_3\rangle = \frac{1}{\sqrt{N_1}}|0\rangle^{\text{Anc.}} \sum_{k=1}^{r} \sigma_k |y_k\rangle_q^L |\sigma_k^2\rangle_q^C (|\boldsymbol{u}_k\rangle|\boldsymbol{\nu}_k\rangle)^B, \tag{8}$$

where $N_1 = \sum_{k=1}^{r} \sigma_k^2$.

Step 4 Rotation. Through rotation transformation $\hat{U}_{\text{c,R}}$, we assign y_k stored in the qumode L to the amplitude of the auxiliary qubit,

$$\begin{aligned} |\psi_4\rangle \;=\; & \frac{1}{\sqrt{N_1}} \sum_{k=1}^{r} \sigma_k [\sin(y_k\alpha)|1\rangle + \cos(y_k\alpha)|0\rangle]^{\text{Anc.}} \\ & \otimes |y_k\rangle^L{}_q |\sigma_k{}^2\rangle_q^C (|\boldsymbol{u}_k\rangle|\boldsymbol{\nu}_k\rangle)^B. \end{aligned} \tag{9}$$

Step 5 $\hat{U}^\dagger$. We perform $\hat{U}^\dagger = \left(I \otimes \hat{U}_{\text{PE}}^\dagger\right)\left(I \otimes U_{\sigma,\tau}^\dagger \otimes I\right)$ on $|\psi_5\rangle$ to eliminate unwanted qumodes L and C,

$$\begin{aligned} |\psi_5\rangle \;=\; & \frac{1}{\sqrt{N_1}} \sum_{k=1}^{r} \sigma_k [\sin(y_k\alpha)|1\rangle + \cos(y_k\alpha)|0\rangle]^{\text{Anc.}} \\ & \times (|\boldsymbol{u}_k\rangle|\boldsymbol{\nu}_k\rangle)^B. \end{aligned} \tag{10}$$

Step 6 Projection measurement. We do projection measurement on the auxiliary qubit and project the quantum state onto $|1\rangle$, then the system collapses to

$$|\psi_6\rangle = \frac{1}{\sqrt{N_\alpha}} \sum_{k=1}^{r} \sigma_k \sin(y_k\alpha)(|\boldsymbol{u}_k\rangle|\boldsymbol{\nu}_k\rangle)^B, \tag{11}$$

where $N_\alpha = \sum_{k=1}^{r} \sigma_k^2 \sin^2(y_k\alpha)$.

4. Algorithm analysis

In this section, we first analyze the space consumption and time complexity of our algorithm and then briefly describe the success probability and fidelity.

4.1. Complexity

To begin with, we focus on the space consumption of our algorithm. In the hybrid quantum phase estimation, register B storing $|\psi_A\rangle$ takes up most space in our algorithm. The number of qubits in register B is $b = O[\log(MN)]$. In addition, we need a few (8 to be precise) qumodes with squeezing factor[14] ε^{-1} for the desired precision ε in the computation of $\hat{U}_{\text{PE}}$, $\hat{U}_{\sigma,\tau}$, and $\hat{U}_{\text{c,R}}$. In contrast, the register consisting of qubits requires $O[\log(\varepsilon^{-1})]$ qubits to register a floating point value. Therefore, we need totally $O[\log(MN)]$ qubits and $O(1)$ qumodes in our hybrid scheme, which is significantly less than the all-qubit QSVT algorithm requiring $O[\log(MN/\varepsilon)]$ qubits. We reduce the number of qubits by replacing the registers widely used in $\hat{U}_{\text{PE}}$, $\hat{U}_{\sigma,\tau}$, and $\hat{U}_{\text{c,R}}$ with qumodes.

We now turn to the runtime analysis. Our hybrid quantum phase estimation is much simplified, only a single operation $\hat{U} = \mathrm{e}^{\mathrm{i}H\hat{P}}$ on $|\psi_A\rangle|0\rangle_q$ is performed, and the singular values are registered into the qumode. However, in the all-qubit scheme, performing quantum Fourier transformation (QFT) on N qubits takes the order of N^2 quantum operations.[1] The number of operations in the computation of $\hat{U}_{\sigma,\tau}$ is a low degree polynomial in the quantity of qumodes. Since the space of qumodes is $O(1)$, $\hat{U}_{\sigma,\tau}$ takes the runtime of $O(1)$. The next operation $\hat{U}_{\text{c,R}}$ is another single gate. Therefore, the total number of operation in our hybrid approach is $O(1)$. While in the all-qubit QSVT algorithm, the number of operation is $O[\text{poly}(\log(1/\varepsilon))]$.

To summarize, our proposed HQSVT algorithm requires $O[\log(MN)]$ qubits and $O(1)$ qumodes, and the runtime is $O(1)$. It is noted that we did not take the runtime for the preparation of intial state $|\psi_A\rangle$ and the time used to construct $\hat{U}_{\text{PE}}$ into account. It costs time $O[\log(MN)]$ via qRAM to prepare state $|\psi_A\rangle$. For desired precision ε, it requires $O(\varepsilon^{-1})$ copies of density matrix $A^{\text{T}}A$, where each copy of density matrix $A^{\text{T}}A$ can be obtained from $|\psi_A\rangle$ in $O[\log(MN)]$ by qRAM. Thus the

total runtime scales as $O[\varepsilon^{-1}\log(MN)]$ and our runtime optimization is limited.

4.2. The success probability and fidelity

We now analyze the probability of obtaining the final result and the fidelity between the ideal and actual results in the same way as the all-qubit approach.

In the first place, the probability of obtaining the final result is calculated as follows:

$$P(\alpha)=\frac{N_\alpha}{N_0}=\frac{\sum_{k=1}^{r}\sigma_k^2\sin^2(y_k\alpha)}{\sum_{k=1}^{R}\sigma_k^2}. \tag{12}$$

Furthermore, we get the fidelity via the inner product between our circuit output $|\psi_S\rangle$ in Eq. (11) and the theoretical output

$$\begin{aligned}|\psi_S'\rangle &= \frac{1}{\sqrt{N_2}}\sum_{k=1}^{r}(\sigma_k-\tau)_+|u_k\rangle|\nu_k\rangle\\ &= \frac{1}{\sqrt{N_2}}\sum_{k=1}^{r}\sigma_k y_k|u_k\rangle|\nu_k\rangle,\end{aligned}$$

where $N_2=\sum_{k=1}^{r}\sigma_k{}^2y_k{}^2$,

$$\begin{aligned}F(\alpha) &= \langle\psi_S|\psi_S'\rangle=\frac{1}{\sqrt{N_2N_\alpha}}\sum_{k=1}^{r}\sigma_k^2y_k\sin(y_k\alpha)\\ &= \frac{\sum_{k=1}^{r}\sigma_k^2y_k\sin(y_k\alpha)}{\sqrt{\sum_{k=1}^{r}\sigma_k^2y_k^2\times\sum_{k=1}^{r}\sigma_k^2\sin^2(y_k\alpha)}}.\end{aligned} \tag{13}$$

According to Cong *et al.*,[30] $y_k\alpha\approx\sin^{-1}(y_k)$. Therefore,

$$P(\alpha)\approx\frac{\sum_{k=1}^{r}\sigma_k^2y_k^2}{\sum_{k=1}^{r}\sigma_k^2}$$

and $F(\alpha)\approx 1$.

5. Conclusion

In this paper, we utilized the advantages of qubits and qumodes in a balanced way and proposed an HQSVT algorithm based on the all-qubit QSVT algorithm. It enables the hybrid quantum computer to solve many NNM-based problems. We decomposed our algorithm into several key subroutines and further investigated the construction of each subroutine through hybrid systems composed of qubits and qumodes. Then we analyzed the space–time complexity of our algorithm, which shows that our algorithm requires $O[\log(MN)]$ qubits and $O(1)$ qumodes, and its runtime is $O(1)$, therefore it is an optimization of the all-qubit QSVT algorithm. In order to register the singular values with the same precision as the all-qubit approach, we take qumodes with squeezing factor ε^{-1} for the desired precision ε, so that our algorithm has the same success probability of obtaining the final result and the fidelity between the ideal and actual outputs. It is worth mentioning that our optimization method is not limited to the QSVT. The proposed method can be applied to other quantum phase estimation-based algorithms, such as quantum principal component analysis and quantum linear regression.

Acknowledgments

Project supported by the Key Research and Development Program of Guangdong Province, China (Grant No. 2018B030326001) and the National Natural Science Foundation of China (Grant Nos. 61521001, 12074179, and 11890704).

References

[1] Nielsen M A and Chuang I L 2010 *Quantum Computation and Quantum Information*, 10th edn. (Cambridge, New York: Cambridge University Press)
[2] Cirac J I and Zoller P 1995 *Phys. Rev. Lett.* **74** 4091
[3] Lau H K and James D F V 2012 *Phys. Rev. A* **85** 062329
[4] Shen C, Zhang Z and Duan L M 2014 *Phys. Rev. Lett.* **112** 050504
[5] Chuang I L, Vandersypen L M K, Zhou X, Leung D W and Lloyd S 1998 *Nature* **393** 143
[6] Jones J A and Mosca M 1998 *J. Chem. Phys.* **109** 1648
[7] Knill E, Laflamme R and Milburn G J 2001 *Nature* **409** 46
[8] Pittman T B, Jacobs B C and Franson J D 2002 *Phys. Rev. Lett.* **88** 257902
[9] Franson J D, Jacobs B C and Pittman T B 2004 *Phys. Rev. A* **70** 062302
[10] Martinis J M and Osborne K 2004 (Preprint cond-mat/0402415)
[11] Blais A, Huang R S, Wallraff A, Girvin S M and Schoelkopf R J 2004 *Phys. Rev. A* **69** 062320
[12] Blais A, Grimsmo A L, Girvin S M and Wallraff A 2021 *Rev. Mod. Phys.* **93** 025005
[13] Krantz P, Kjaergaard M, Yan F, Orlando T P, Gustavsson S and Oliver W D 2019 *Appl. Phys. Rev.* **6** 021318
[14] Liu N, Thompson J, Weedbrook C, Lloyd S, Vedral V, Gu M and Modi K 2016 *Phys. Rev. A* **93** 052304
[15] Lloyd S 2003 *Hybrid quantum computing, in Quantum Information with Continuous Variables* (Dordrecht: Springer)
[16] van Loock P, Munro W J, Nemoto K, Spiller T P, Ladd T D, Braunstein S L and Milburn G J 2008 *Phys. Rev. A* **78** 022303
[17] Lloyd S and Braunstein S L 1999 *Phys. Rev. Lett.* **82** 1784
[18] Jolliffe I T 2002 *Principal Component Analysis* (Springer)
[19] Lloyd S, Mohseni M and Rebentrost P 2014 *Nat. Phys.* **10** 631
[20] Lin J, Bao W S, Zhang S, Li T and Wang X 2019 *Phys. Lett. A* **383** 2862
[21] Biamonte J, Wittek P, Pancotti N, Rebentrost P, Wiebe N and Lloyd S 2017 *Nature* **549** 195
[22] Duan B, Yuan J, Liu Y and Li D 2018 *Phys. Rev. A* **98** 012308
[23] Duan B, Yuan J, Liu Y and Li D 2017 *Phys. Rev. A* **96** 032301
[24] Harrow A W, Hassidim A and Lloyd S 2009 *Phys. Rev. Lett.* **103** 150502
[25] Giovannetti V, Lloyd S and Maccone L 2008 *Phys. Rev. A* **78** 052310
[26] Hong F Y, Xiang Y, Zhu Z Y, Jiang L Z and Wu L N 2012 *Phys. Rev. A* **86** 010306
[27] Patton K R and Fischer U R 2013 *Phys. Rev. Lett.* **111** 240504
[28] Lau H K and Plenio M B 2016 *Phys. Rev. Lett.* **117** 100501
[29] Vedral V, Barenco A and Ekert A 1996 *Phys. Rev. A* **54** 147
[30] Cong I and Duan L 2016 *New J. Phys.* **18** 073011